Operational formulation of weak values without probe systems

Kazuhisa Ogawa,[1,*] Hirokazu Kobayashi[2] and Akihisa Tomita[1]

[1]*Graduate School of Information Science and Technology, Hokkaido University, Sapporo 060-0814, Japan*
[2]*School of System Engineering, Kochi University of Technology, Tosayamada-cho, Kochi 782-8502, Japan*

Weak values are the fundamental values for observables in a pre- and postselected system. Weak values are typically measured by weak measurement, in which weak values appear in the change of not the pre- and postselected system but the probe system. This indirect characteristic of weak measurement obscures the meaning of weak values for the pre- and postselected system, in contrast to conventional physical quantities, which have a clear operational meaning. In this study, we operationally formulate weak values as the sensitivity of postselection probability amplitude to small transformation in a pre- and postselected system. This formulation of weak values, which is free from the concept of probe shift assumed in weak measurement, gives a direct interpretation of strange weak values for the pre- and postselected system. Furthermore, this formulation can simplify weak-value measurement experiments because the associated measurements appearing in the modulus change of the postselection probability amplitude do not require external degrees of freedom.

I. INTRODUCTION

For an observable $\hat{A}$, a quantum system pre- and postselected in $|i\rangle$ and $|f\rangle$, respectively, has a complex characteristic value called *weak value*:

$$\langle\hat{A}\rangle_{\mathrm{w}} := \frac{\langle f|\hat{A}|i\rangle}{\langle f|i\rangle}. \tag{1}$$

The weak value was originally introduced as a measurement outcome of *weak measurement* for a pre- and postselected system [1]. In weak measurement, an additional degree of freedom is employed as a probe system besides the pre- and postselected system to be measured. A preselected system $|i\rangle$ weakly interacts with the probe system and is then postselected in $|f\rangle$; after postselection, the weak value is obtained as a position and momentum shifts of the probe system [2]. Weak measurement has been used to study various fundamental problems in quantum mechanics [3–10] because it provides weak values as intermediate information of the pre- and postselected systems without disturbing them. In addition, weak measurement has been applied for precise measurements of magnitudes of weak system–probe interactions (weak-value amplification) [11–14], as well as direct measurements of wave functions and pseudoprobability distributions of the system's preselected state [15–22].

Weak values can be beyond the range of the observable's eigenvalues, a fact that has been one of the central topics in weak values and weak measurement [1,3–6,11–14]. Such "strange weak values" [23] are intriguing when regarded as an extension of conventional physical quantities, such as classical physical quantities and quantum expectation values. However, there is a difference between the weak values obtained by weak measurement and the conventional physical

quantities in terms of the directness of the measurement procedure. The conventional physical quantities can be directly measured from the state changes of the measured system itself, and probe systems are not necessarily required. In contrast, in weak measurement, weak values are observed not in the changes of the pre- and postselected system but in the shifts of the probe system. This indirect characteristic of weak measurement makes it difficult to consider weak values as a naive extension of conventional physical quantities and obscures what the weak values represent for the pre- and postselected system. Because weak values inherently belong to the pre- and postselected system [24], they should be observed in that system's changes.

In this study, we operationally formulate weak values as the sensitivity of the pre- and postselected system to a small transformation, such as unitary and amplification or attenuation transformations. The weak value of the derivative of the small transformation is observed as the response of the postselection probability amplitude change. This relation also holds for conventional physical quantities; therefore, this formulation allows us to interpret weak values as a natural extension of the conventional physical quantities regardless of the presence of the probe systems. We apply this formulation to cases of the quantum box problem [3,4] and the huge weak value of spin [1] as examples and examine how the strange weak values can be directly understood as a natural extension of the conventional physical quantities such as probability and spin angular momentum.

In addition, the weak values appearing in the modulus change of the postselection probability amplitude in this formulation can be measured directly using the system without the need for external degrees of freedom. Therefore, the weak-value measurements based on this formulation are easier to implement than conventional weak measurements, which require the preparation and measurement of the probe system. We discuss the applicability of this simple weak-value

*ogawak@ist.hokudai.ac.jp

measurement method and evaluate its performance in terms of accuracy and precision.

This paper is organized as follows. In Sec. II, we introduce an operational formulation of weak values and explain how to obtain the real and imaginary parts of weak values experimentally in this formulation. In Sec. III, we apply this formulation to the cases of the quantum box problem and the huge weak value of spin as examples. In Sec. IV, we examine the performance of this method to show that it can be used to simplify measurement experiments for various applications of weak values. Finally, we summarize the findings of our study in Sec. V.

II. OPERATIONAL FORMULATION OF WEAK VALUES WITHOUT PROBE SYSTEMS

In this section, we operationally formulate the weak values as the sensitivity of the postselection probability amplitude when a small transformation is set between the pre- and postselection. In Sec. II A, we first introduce a small linear transformation and provide the general theory of this formulation. In Secs. II B and II C, we describe how to obtain real and imaginary parts of weak values in this formulation, respectively. In Sec. II D, we extend this formulation to the case of the mixed pre- and postselection and that of the preselection only. In Sec. II E, we mention the previous studies related to this formulation of weak values.

A. General theory

To derive an operational formulation of the weak value of a normal operator $\hat{C}$ for a pre- and postselected system, we first introduce the following small linear transformation $\hat{N}(\theta)$. $\hat{N}(\theta)$ is a normal operator parametrized by a small real parameter θ, which maps a pure state onto another pure state. We assume that $\hat{N}(\theta)$ satisfies $\hat{N}(0) = \hat{1}$ and can be expanded for θ as [25]

$$\hat{N}(\theta) = \hat{1} + \theta\hat{C} + O(\theta^2). \quad (2)$$

$\hat{C}$ is the derivative of $\hat{N}(\theta)$ at $\theta = 0$, and we call $\hat{C}$ the *generator* of $\hat{N}(\theta)$. While the exponential form $\exp(\theta\hat{C})$ is an example of $\hat{N}(\theta)$, we do not limit $\hat{N}(\theta)$ to the exponential form here.

We next consider the pre- and postselected systems $\{|i\rangle, |f\rangle\}$ shown in Figs. 1(a) and 1(b). In the system of Fig. 1(b), a small linear transformation $\hat{N}(\theta)$ is set between the pre- and postselection. After the postselection, the output states have postselection probability amplitudes $\langle f|i\rangle$ and $\langle f|\hat{N}(\theta)|i\rangle$. We evaluate the sensitivity of $\langle f|\hat{N}(\theta)|i\rangle$ to θ by the ratio of $\langle f|\hat{N}(\theta)|i\rangle$ to $\langle f|i\rangle$.

This ratio can be expanded for θ as

$$\frac{\langle f|\hat{N}(\theta)|i\rangle}{\langle f|i\rangle} = 1 + \langle\hat{C}\rangle_w\theta + O(\theta^2). \quad (3)$$

This equation indicates that the derivative of this ratio for θ at $\theta = 0$ corresponds to the weak value of $\hat{C}$:

$$\frac{d}{d\theta}\frac{\langle f|\hat{N}(\theta)|i\rangle}{\langle f|i\rangle}\bigg|_{\theta=0} = \langle\hat{C}\rangle_w. \quad (4)$$
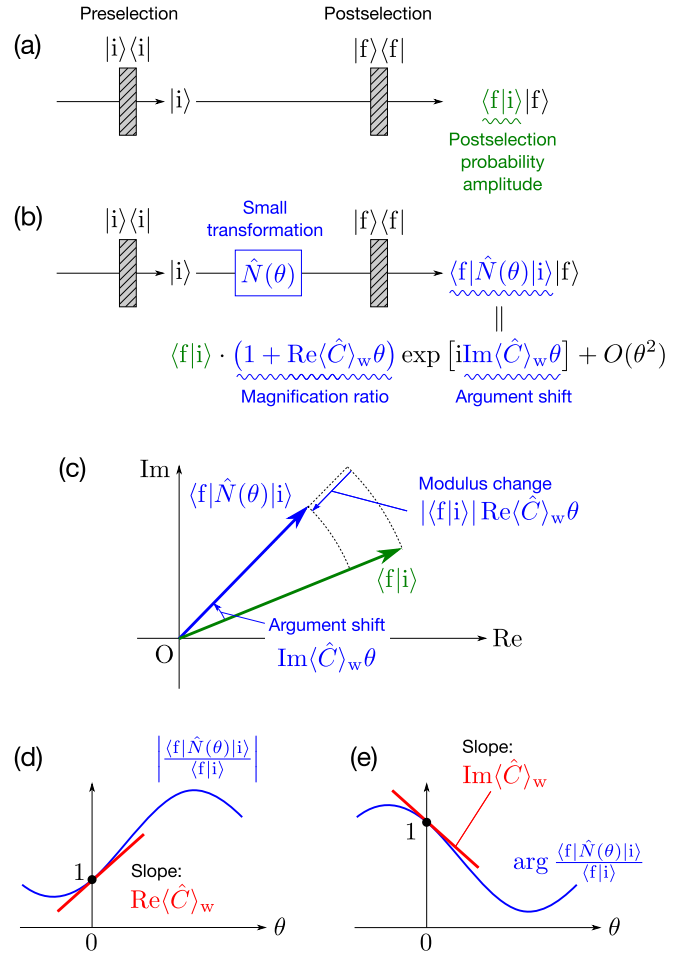

FIG. 1. Schematic overview of the proposed operational formulation of weak values. (a) Pre- and postselected system $\{|i\rangle, |f\rangle\}$. The postselected state has a postselection probability amplitude $\langle f|i\rangle$. (b) The pre- and postselected system that includes a small transformation $\hat{N}(\theta)$. For its postselection probability amplitude $\langle f|\hat{N}(\theta)|i\rangle$, its modulus is magnified $1 + \text{Re}\langle\hat{C}\rangle_w\theta$ times, and its argument is shifted by $\text{Im}\langle\hat{C}\rangle_w\theta$ compared with $\langle f|i\rangle$. (c) Relation between $\langle f|i\rangle$ and $\langle f|\hat{N}(\theta)|i\rangle$ on the complex plane. The real and imaginary parts of $\langle\hat{C}\rangle_w$ appear in the differences of the modulus and the argument between them, respectively. The higher-order term $O(\theta^2)$ is not displayed here. (d) Relation between $|\langle f|\hat{N}(\theta)|i\rangle/\langle f|i\rangle|$ and $\text{Re}\langle\hat{C}\rangle_w$. $\text{Re}\langle\hat{C}\rangle_w$ is represented as the slope of $|\langle f|\hat{N}(\theta)|i\rangle/\langle f|i\rangle|$ at $\theta = 0$. (e) Relation between $\arg[\langle f|\hat{N}(\theta)|i\rangle/\langle f|i\rangle]$ and $\text{Im}\langle\hat{C}\rangle_w$. $\text{Im}\langle\hat{C}\rangle_w$ is represented as the slope of $\arg[\langle f|\hat{N}(\theta)|i\rangle/\langle f|i\rangle]$ at $\theta = 0$.

In other words, for the pre- and postselected system $\{|i\rangle, |f\rangle\}$, $\langle\hat{C}\rangle_w$ is formulated as the sensitivity (i.e., rate of change) of the postselection probability amplitude to the small transformation whose generator is $\hat{C}$.

Moreover, Eqs. (3) and (4) can be rewritten as [26]

$$\frac{\langle f|\hat{N}(\theta)|i\rangle}{\langle f|i\rangle} = (1 + \text{Re}\langle\hat{C}\rangle_w\theta)\exp[i\,\text{Im}\langle\hat{C}\rangle_w\theta] + O(\theta^2), \quad (5)$$

$$\frac{d}{d\theta}\left|\frac{\langle f|\hat{N}(\theta)|i\rangle}{\langle f|i\rangle}\right|\bigg|_{\theta=0} = \text{Re}\langle\hat{C}\rangle_w, \quad (6)$$

$$\frac{d}{d\theta}\arg\frac{\langle f|\hat{N}(\theta)|i\rangle}{\langle f|i\rangle}\bigg|_{\theta=0} = \text{Im}\langle\hat{C}\rangle_w. \quad (7)$$

TABLE I. Relations between each type of small transformation and the variation of the modulus and argument of $\langle f|\hat{N}(\theta)|i\rangle$.

Small transformation	Variation of Modulus	$\langle f|\hat{N}(\theta)|i\rangle$: Argument
Unitary: $\hat{U}(\theta) = \hat{1} + i\theta\hat{A} + O(\theta^2)$	$-|\langle f|i\rangle|\text{Im}\langle\hat{A}\rangle_w\theta$	$\text{Re}\langle\hat{A}\rangle_w\theta$
Amplification or attenuation: $\hat{T}(\theta) = \hat{1} + \theta\hat{B} + O(\theta^2)$	$|\langle f|i\rangle|\text{Re}\langle\hat{B}\rangle_w\theta$	$\text{Im}\langle\hat{B}\rangle_w\theta$

Equation (5) means that the modulus of $\langle f|\hat{N}(\theta)|i\rangle$ is magnified $1 + \text{Re}\langle\hat{C}\rangle_w\theta$ times, and its argument is shifted by $\text{Im}\langle\hat{C}\rangle_w\theta$ compared with $\langle f|i\rangle$. This relation is depicted on the complex plane shown in Fig. 1(c). Equations (6) and (7) mean that the real and imaginary parts of $\langle\hat{C}\rangle_w$ are formulated as the sensitivity of the variation of the modulus and argument of the postselection probability amplitude. The relations between $|\langle f|\hat{N}(\theta)|i\rangle/\langle f|i\rangle|$ and $\text{Re}\langle\hat{C}\rangle_w$ and between $\arg[\langle f|\hat{N}(\theta)|i\rangle/\langle f|i\rangle]$ and $\text{Im}\langle\hat{C}\rangle_w$ are depicted in Figs. 1(d) and 1(e), respectively.

The remainder of this section notes the special cases of the small transformation $\hat{N}(\theta)$. The generator $\hat{C}$ is expressed using two Hermite operators $\hat{A}$ and $\hat{B}$ as $\hat{C} = i\hat{A} + \hat{B}$. When $\hat{C} = i\hat{A}$, $\hat{N}(\theta)$ becomes a unitary transformation $\hat{U}(\theta) := \hat{1} + i\theta\hat{A} + O(\theta^2)$ in the first-order approximation of θ. In contrast, when $\hat{C} = \hat{B}$, $\hat{N}(\theta)$ becomes an amplification or attenuation transformation $\hat{T}(\theta) := \hat{1} + \theta\hat{B} + O(\theta^2)$, which amplifies (attenuates) the moduli of the amplitudes in the eigenspaces of $\hat{B}$ whose eigenvalues are positive (negative) when $\theta > 0$ (how to realize the amplification or attenuation transformation by unitary processes is explained in Appendix A). Because of the following relations:

$$\text{Re}\langle\hat{C}\rangle_w = -\text{Im}\langle\hat{A}\rangle_w + \text{Re}\langle\hat{B}\rangle_w, \quad (8)$$

$$\text{Im}\langle\hat{C}\rangle_w = \text{Re}\langle\hat{A}\rangle_w + \text{Im}\langle\hat{B}\rangle_w, \quad (9)$$

$\text{Re}\langle\hat{A}\rangle_w$, $\text{Im}\langle\hat{A}\rangle_w$, $\text{Re}\langle\hat{B}\rangle_w$, and $\text{Im}\langle\hat{B}\rangle_w$ appear in the variation of $\langle f|\hat{N}(\theta)|i\rangle$ as shown in Table I.

B. How to obtain $\text{Re}\langle\hat{C}\rangle_w$ experimentally

This section and the next section describe how to obtain $\text{Re}\langle\hat{C}\rangle_w$ and $\text{Im}\langle\hat{C}\rangle_w$ experimentally, respectively. According to Eqs. (5) and (6), $\text{Re}\langle\hat{C}\rangle_w$ appears in the modulus of $\langle f|\hat{N}(\theta)|i\rangle/\langle f|i\rangle$. The square of this modulus can be obtained by measuring the postselection probability $P(f|i, \theta) := |\langle f|\hat{N}(\theta)|i\rangle|^2$ by the system shown in Fig. 2(a) as

$$\frac{P(f|i, \theta)}{P(f|i, 0)} = \frac{|\langle f|\hat{N}(\theta)|i\rangle|^2}{|\langle f|\hat{N}(0)|i\rangle|^2} = \left|\frac{\langle f|\hat{N}(\theta)|i\rangle}{\langle f|i\rangle}\right|^2. \quad (10)$$

Therefore, $\text{Re}\langle\hat{C}\rangle_w$ can be obtained experimentally by measuring the postselection probability $P(f|i, \theta)$ for $\theta = 0$ and $\theta \neq 0$ as

$$\frac{P(f|i, \theta)}{P(f|i, 0)} = 1 + 2\text{Re}\langle\hat{C}\rangle_w\theta + O(\theta^2), \quad (11)$$

$$\left.\frac{d}{d\theta}\frac{P(f|i, \theta)}{P(f|i, 0)}\right|_{\theta=0} = 2\text{Re}\langle\hat{C}\rangle_w. \quad (12)$$
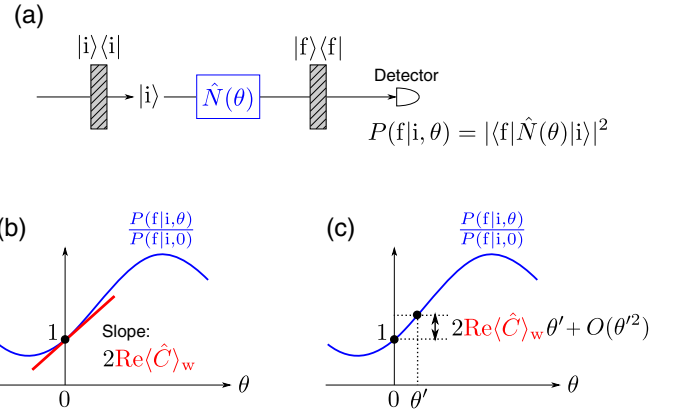

FIG. 2. (a) Schematic diagram of the pre- and postselected system for measuring $\text{Re}\langle\hat{C}\rangle_w$. (b),(c) Relation between $P(f|i, \theta)/P(f|i, 0)$ and $\text{Re}\langle\hat{C}\rangle_w$. (b) $\text{Re}\langle\hat{C}\rangle_w$ is represented as a half of the slope of $P(f|i, \theta)/P(f|i, 0)$ at $\theta = 0$. (c) Experimentally, $\text{Re}\langle\hat{C}\rangle_w$ is obtained as the difference between 1 and $P(f|i, \theta')/P(f|i, 0)$ for small θ'.

The relation between $P(f|i, \theta)/P(f|i, 0)$ and $\text{Re}\langle\hat{C}\rangle_w$ is illustrated in Figs. 2(b) and 2(c). Equation (12) indicates that $\text{Re}\langle\hat{C}\rangle_w$ is represented as the slope of $P(f|i, \theta)/P(f|i, 0)$ at $\theta = 0$. Experimentally, $\text{Re}\langle\hat{C}\rangle_w$ is obtained as the difference between 1 and $P(f|i, \theta)/P(f|i, 0)$ for small θ. Remarkably, this method to obtain $\text{Re}\langle\hat{C}\rangle_w$ does not require a probe system, which is unlike conventional weak measurement. As Eq. (8) indicates, $\text{Re}\langle\hat{C}\rangle_w = \text{Re}\langle\hat{A}\rangle_w$ when $\hat{C} = \hat{A}$, and $\text{Re}\langle\hat{C}\rangle_w = -\text{Im}\langle\hat{A}\rangle_w$ when $\hat{C} = i\hat{A}$, for a Hermite operator $\hat{A}$. Therefore, both the real and imaginary parts of the weak value for the desired Hermite operator $\hat{A}$ can be obtained experimentally without using probe systems. This characteristic can be a practical advantage for weak-value measurement experiments and will be discussed in Sec. IV.

C. How to obtain $\text{Im}\langle\hat{C}\rangle_w$ experimentally

Next, we describe how to obtain $\text{Im}\langle\hat{C}\rangle_w$ experimentally in this formulation. According to Eqs. (5) and (7), $\text{Im}\langle\hat{C}\rangle_w$ appears in the argument of $\langle f|\hat{N}(\theta)|i\rangle/\langle f|i\rangle$. This argument can be obtained experimentally by measuring the phase difference between $\arg\langle f|\hat{N}(\theta)|i\rangle$ for $\theta \neq 0$ and $\theta = 0$ as

$$\arg\langle f|\hat{N}(\theta)|i\rangle - \arg\langle f|\hat{N}(0)|i\rangle = \arg\frac{\langle f|\hat{N}(\theta)|i\rangle}{\langle f|i\rangle}$$
$$= \text{Im}\langle\hat{C}\rangle_w\theta + O(\theta^2). \quad (13)$$

This argument shift, which appears in the global phase of the postselected state, cannot be measured experimentally with only the system shown in Fig. 2(a); however, using an interferometer for another degree of freedom as in Figs. 3(a) and 3(b), we can measure it experimentally. The added external degree of freedom is depicted as the path mode in the interferometer. The internal degrees of freedom are pre- and postselected to $|i\rangle$ and $|f\rangle$, respectively, and, in the upper path, the small linear transformation $\hat{N}(\theta)$ is set between the pre- and postselection. The relative phase δ in the interferometer is varied by the phase shifter $e^{i\delta}$ in the lower path. The
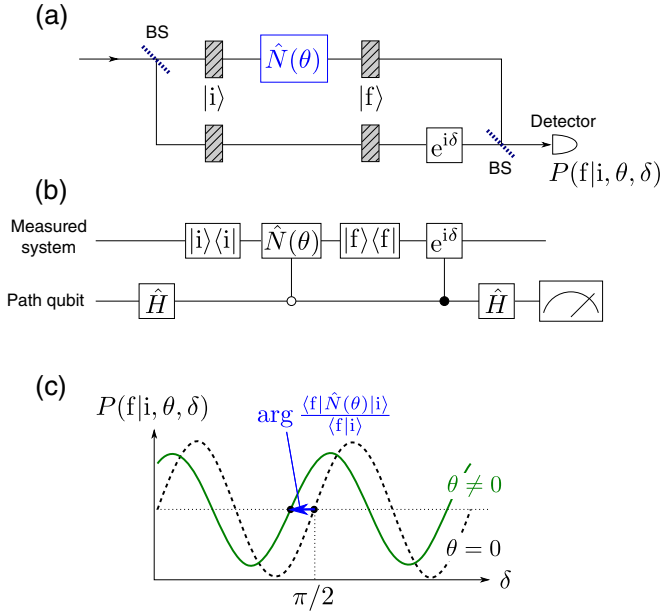
FIG. 3. (a) Schematic diagram of the interferometer for measuring $\mathrm{Im}\langle\hat{C}\rangle_{\mathrm{w}}$. The upper and lower path modes in the interferometer show the added external degrees of freedom. BS: beam splitter, which works as a Hadamard operator for the external degrees of freedom. (b) Quantum circuit representation of the interferometer (a). (c) Variation of the detection probability $P(\mathrm{f}|\mathrm{i},\theta,\delta)$ with respect to δ. The black dashed and green solid lines are the cases for $\theta=0$ and $\theta\neq0$, respectively. The phase shift of the interference fringes corresponds to $\arg[\langle\mathrm{f}|\hat{N}(\theta)|\mathrm{i}\rangle/\langle\mathrm{f}|\mathrm{i}\rangle]$, which approximately equals $\mathrm{Im}\langle\hat{C}\rangle_{\mathrm{w}}$.

postselection probability $P(\mathrm{f}|\mathrm{i},\theta,\delta)$ is expressed as

$$
P(\mathrm{f}|\mathrm{i},\theta,\delta) = \frac{|\langle\mathrm{f}|\mathrm{i}\rangle|^2}{4}\left\{ \left|\frac{\langle\mathrm{f}|\hat{N}(\theta)|\mathrm{i}\rangle}{\langle\mathrm{f}|\mathrm{i}\rangle}\right|^2 + 1 \right.
$$
$$
\left. + \left|\frac{\langle\mathrm{f}|\hat{N}(\theta)|\mathrm{i}\rangle}{\langle\mathrm{f}|\mathrm{i}\rangle}\right| 2\cos\left[\delta - \arg\frac{\langle\mathrm{f}|\hat{N}(\theta)|\mathrm{i}\rangle}{\langle\mathrm{f}|\mathrm{i}\rangle}\right]\right\},
$$
(14)

which exhibits interference fringes with respect to δ. For $\theta\neq0$, the phase of the interference fringe is displaced by $\arg[\langle\mathrm{f}|\hat{N}(\theta)|\mathrm{i}\rangle/\langle\mathrm{f}|\mathrm{i}\rangle]$ from that for $\theta=0$, and the slope of $\arg[\langle\mathrm{f}|\hat{N}(\theta)|\mathrm{i}\rangle/\langle\mathrm{f}|\mathrm{i}\rangle]$ at $\theta=0$ corresponds to $\mathrm{Im}\langle\hat{C}\rangle_{\mathrm{w}}$, as shown in Fig. 3(c). Therefore, $\mathrm{Im}\langle\hat{C}\rangle_{\mathrm{w}}$ can be obtained by measuring the interference fringe's phase shift $\arg[\langle\mathrm{f}|\hat{N}(\theta)|\mathrm{i}\rangle/\langle\mathrm{f}|\mathrm{i}\rangle]$ for small θ. We note that measurement of $\mathrm{Im}\langle\hat{C}\rangle_{\mathrm{w}}$ requires another degree of freedom, which corresponds to a probe system in conventional weak measurement, whereas the formulation of $\mathrm{Im}\langle\hat{C}\rangle_{\mathrm{w}}$ in Eq. (7), i.e., how it appears in mathematical formulas, does not require it.

D. Case of mixed pre- and postselection and that of preselection only

Here, we extend the proposed operational formulation of weak values to the case of the mixed pre- and postselection. Then, we use this extended formulation to show that the expectation values for a preselected system are formulated in

the same form as the weak values for a pre- and postselected system. This relation indicates that the weak values are natural extensions of the expected values, regardless of the presence of the probe systems.

The weak value of $\hat{C}$ for the system pre- and postselected in the mixed states $\hat{\rho}_{\mathrm{i}}$ and $\hat{\rho}_{\mathrm{f}}$, respectively, is given as

$$
\langle\hat{C}\rangle_{\mathrm{w}} = \frac{\mathrm{tr}(\hat{\rho}_{\mathrm{f}}\hat{C}\hat{\rho}_{\mathrm{i}})}{\mathrm{tr}(\hat{\rho}_{\mathrm{f}}\hat{\rho}_{\mathrm{i}})}.
$$
(15)

The formulation proposed in Sec. II A appears to not be suitable for this case because the postselection probability amplitude is not defined for mixed states. However, the measurement methods introduced in Secs. II B and II C also work to observe the real and imaginary parts of the weak values even for the case of the mixed pre- and postselection. In the system shown in Fig. 2(a), the postselection probability for the pre- and postselection $\{\hat{\rho}_{\mathrm{i}},\hat{\rho}_{\mathrm{f}}\}$ is given as $P(\mathrm{f}|\mathrm{i},\theta) = \mathrm{tr}[\hat{\rho}_{\mathrm{f}}\hat{N}(\theta)\hat{\rho}_{\mathrm{i}}\hat{N}^{\dagger}(\theta)]$. Therefore, the following relation same as Eq. (12) holds:

$$
\left.\frac{d}{d\theta}\frac{P(\mathrm{f}|\mathrm{i},\theta)}{P(\mathrm{f}|\mathrm{i},0)}\right|_{\theta=0} = \left.\frac{d}{d\theta}\frac{\mathrm{tr}[\hat{\rho}_{\mathrm{f}}\hat{N}(\theta)\hat{\rho}_{\mathrm{i}}\hat{N}^{\dagger}(\theta)]}{\mathrm{tr}(\hat{\rho}_{\mathrm{f}}\hat{\rho}_{\mathrm{i}})}\right|_{\theta=0} = 2\,\mathrm{Re}\langle\hat{C}\rangle_{\mathrm{w}}.
$$
(16)

Similarly, the postselection probability in the system shown in Fig. 3(a) is given as

$$
P(\mathrm{f}|\mathrm{i},\theta,\delta) = \frac{\mathrm{tr}(\hat{\rho}_{\mathrm{f}}\hat{\rho}_{\mathrm{i}})}{4}\left\{\frac{\mathrm{tr}[\hat{\rho}_{\mathrm{f}}\hat{N}(\theta)\hat{\rho}_{\mathrm{i}}\hat{N}^{\dagger}(\theta)]}{\mathrm{tr}(\hat{\rho}_{\mathrm{f}}\hat{\rho}_{\mathrm{i}})} + 1\right.
$$
$$
\left. + \left|\frac{\mathrm{tr}[\hat{\rho}_{\mathrm{f}}\hat{N}(\theta)\hat{\rho}_{\mathrm{i}}]}{\mathrm{tr}(\hat{\rho}_{\mathrm{f}}\hat{\rho}_{\mathrm{i}})}\right|2\cos\left[\delta - \arg\frac{\mathrm{tr}[\hat{\rho}_{\mathrm{f}}\hat{N}(\theta)\hat{\rho}_{\mathrm{i}}]}{\mathrm{tr}(\hat{\rho}_{\mathrm{f}}\hat{\rho}_{\mathrm{i}})}\right]\right\}.
$$
(17)

The phase difference between the interference fringes when $\theta\neq0$ and those when $\theta=0$, $\arg\{\mathrm{tr}[\hat{\rho}_{\mathrm{f}}\hat{N}(\theta)\hat{\rho}_{\mathrm{i}}]/\mathrm{tr}(\hat{\rho}_{\mathrm{f}}\hat{\rho}_{\mathrm{i}})\}$, shows the following relation same as Eq. (7):

$$
\left.\frac{d}{d\theta}\arg\frac{\mathrm{tr}[\hat{\rho}_{\mathrm{f}}\hat{N}(\theta)\hat{\rho}_{\mathrm{i}}]}{\mathrm{tr}(\hat{\rho}_{\mathrm{f}}\hat{\rho}_{\mathrm{i}})}\right|_{\theta=0} = \mathrm{Im}\langle\hat{C}\rangle_{\mathrm{w}}.
$$
(18)

As a special case of the mixed pre- and postselection, postselection in the completely mixed state $\hat{1}/d$ (d is the dimension of the system) corresponds to the case of the preselection only. Especially, when the preselected state is a pure state $\hat{\rho}_{\mathrm{i}} = |\mathrm{i}\rangle\langle\mathrm{i}|$, Eq. (16) becomes

$$
\left.\frac{d}{d\theta}\frac{\|\hat{N}(\theta)|\mathrm{i}\rangle\|}{\||\mathrm{i}\rangle\|}\right|_{\theta=0} = \mathrm{Re}\langle\mathrm{i}|\hat{C}|\mathrm{i}\rangle.
$$
(19)

This equation means that the real part of the expectation value of $\hat{C}$ for the preselected state $|\mathrm{i}\rangle$ appears in the sensitivity to θ of the ratio of the norms of $\hat{N}(\theta)|\mathrm{i}\rangle$ for $\theta\neq0$ and $\theta=0$. The formulation of $\mathrm{Re}\langle\hat{C}\rangle_{\mathrm{w}}$ in Eq. (6), which seems to have a different form from that of Eq. (19), can also be rewritten as the ratio of the norms after the postselection as

$$
\left.\frac{d}{d\theta}\frac{\|\langle\mathrm{f}|\hat{N}(\theta)|\mathrm{i}\rangle|\mathrm{f}\rangle\|}{\|\langle\mathrm{f}|\mathrm{i}\rangle|\mathrm{f}\rangle\|}\right|_{\theta=0} = \mathrm{Re}\langle\hat{C}\rangle_{\mathrm{w}}.
$$
(20)

Besides, Eq. (18) for the preselected system $|\mathrm{i}\rangle$ becomes

$$
\left.\frac{d}{d\theta}\arg\langle\mathrm{i}|[\hat{N}(\theta)|\mathrm{i}\rangle]\right|_{\theta=0} = \mathrm{Im}\langle\mathrm{i}|\hat{C}|\mathrm{i}\rangle.
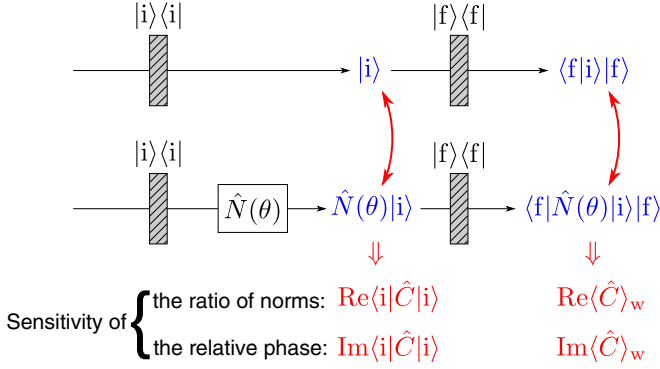$$
(21)

FIG. 4. Unified interpretation of the expectation values and the weak values in our formulation. The real (imaginary) part of the expectation values appears in the sensitivity of the ratio of norms (the relative phase) of the states with and without a small transformation in the preselected system. This formulation using the ratio of norms and the relative phase can also be applied to weak values in the pre- and postselected system.

This equation indicates that the imaginary part of the expectation value $\langle \hat{C} \rangle$ appears in the sensitivity to θ of the relative phase of $\hat{N}(\theta)|\mathrm{i}\rangle$ to $|\mathrm{i}\rangle$, where the relative phase of $|\psi\rangle$ to $|\phi\rangle$ is defined as $\arg\langle\phi|\psi\rangle$ [27]. The formulation of $\mathrm{Im}\langle\hat{C}\rangle_{\mathrm{w}}$ in Eq. (7) can also be rewritten as the sensitivity of the relative phase after the postselection as

$$\frac{d}{d\theta}\arg[\langle\mathrm{f}|\langle\mathrm{i}|\mathrm{f}\rangle][\langle\mathrm{f}|\hat{N}(\theta)|\mathrm{i}\rangle|\mathrm{f}\rangle]|_{\theta=0} = \mathrm{Im}\langle\hat{C}\rangle_{\mathrm{w}}. \quad (22)$$

In this manner, a unified interpretation of the expectation values and the weak values is given in our formulation, as shown in Fig. 4, and the weak values are interpreted as natural extensions of the expected values in our formulation, which requires no probe systems.

E. Related previous studies and difference of our formulation

The operational formulation of weak values as the sensitivity of the system to a small transformation has been mentioned partially in previous studies [9,28–34]. Our formulation described so far is a generalization of them. Here, we refer to each of them and explain the difference of our formulation.

The relation between the modulus change of postselection probability amplitude and the weak value of the generator of the small transformation in Eq. (6) [or Eq. (12)] has been mentioned in Refs. [9,28–33]. References [28–32] assume that the small transformation is the unitary transformation in the form of $\exp(i\theta\hat{A})$ and show that $\mathrm{Im}\langle\hat{A}\rangle_{\mathrm{w}}$ appears in the modulus change of postselection probability amplitude. References [9,29] assume the attenuation transformation in the form of $\exp(\theta\hat{B})$ and show that $\mathrm{Re}\langle\hat{B}\rangle_{\mathrm{w}}$ appears there. In contrast, the relation between the argument shift of postselection probability amplitude and the weak value of the generator of the small transformation in Eq. (7) has been mentioned in Refs. [30,33,34]. These studies assume that the small transformation is the unitary transformation in the form of $\exp(i\theta\hat{A})$ and show that $\mathrm{Re}\langle\hat{A}\rangle_{\mathrm{w}}$ appears in the argument shift of postselection probability amplitude. Also, we note that Refs. [9,28,29,32,34] do not assume the use of probe systems

like our formulation, whereas Refs. [30,31,33] assume the von Neumann interaction with probe systems.

Compared with the related previous studies, our formulation of weak values has the following difference. (i) A small transformation is considered to be not only the unitary transformation $\exp(i\theta\hat{A})$ and the attenuation transformation $\exp(\theta\hat{B})$ but also the general form of Eq. (2). It includes, for example, a mixture of the unitary and attenuation transformations, an amplification transformation, and a linearly parametrized attenuation transformation $\hat{1} - \theta\hat{C}$. (ii) It is noteworthy that when a small amplification or attenuation transformation $\hat{1} + \theta\hat{B} + O(\theta^2)$ is set between pre- and postselection, the imaginary part of the weak value of $\hat{B}$ appears in the argument shift of the postselection probability amplitude, as shown in the bottom right of Table I. (iii) Our formulation is applicable to the systems pre- and postselected in mixed states, which include preselected-only systems. Consequently, the weak values are interpreted as natural extensions of the expected values even without probe systems.

III. EXAMPLES OF DIRECT INTERPRETATION OF STRANGE WEAK VALUES BY THE OPERATIONAL FORMULATION

In this section, we apply our formulation of weak values to the examples of the strange weak values. We deal with the case of the quantum box problem [3,4] in Sec. III A, and the case of the huge weak value of the spin of a spin-1/2 particle [1] in Sec. III B. In both sections, we explain how the conventional physical quantities—classical physical quantities and/or quantum expectation values—and the weak values are interpreted directly by our formulation.

A. Case of quantum box problem

Here, we analyze the quantum box problem using a small attenuation transformation, as an example of the case where the real part of the weak value appears in the sensitivity of the postselection probability mentioned in Sec. II B. The quantum box problem was proposed as a gedanken experiment where a pre- and postselected system shows a curious result [3] and, later, its three box version (three box problem) was experimentally demonstrated using optical weak measurement [4]. In the three box problem, the particle can be a superposition of three orthogonal path states $|A\rangle$, $|B\rangle$, and $|C\rangle$. When the particle is pre- and postselected in $|\mathrm{i}\rangle = (|A\rangle + |B\rangle + |C\rangle)/\sqrt{3}$ and $|\mathrm{f}\rangle = (|A\rangle + |B\rangle - |C\rangle)/\sqrt{3}$, respectively, the weak values of the projection operators of the paths, which are called *weak probabilities*, become

$$\langle|A\rangle\langle A|\rangle_{\mathrm{w}} = \langle|B\rangle\langle B|\rangle_{\mathrm{w}} = 1, \quad \langle|C\rangle\langle C|\rangle_{\mathrm{w}} = -1. \quad (23)$$

Unlike ordinary probabilities, the weak probabilities can be arbitrary complex values out of [0,1] while satisfying that the sum of them is one. Here, we explain that in the proposed formulation, such strange weak probabilities can also be understood in a similar way to the existence probabilities of particles in classical and preselected quantum systems.

First, let us consider the classical pre- and postselected system shown in 5(a), in which the particle is prepared in the path j with a probability of $p_{\mathrm{i},j}$ ($\sum_j p_{\mathrm{i},j} = 1$) at preselection and
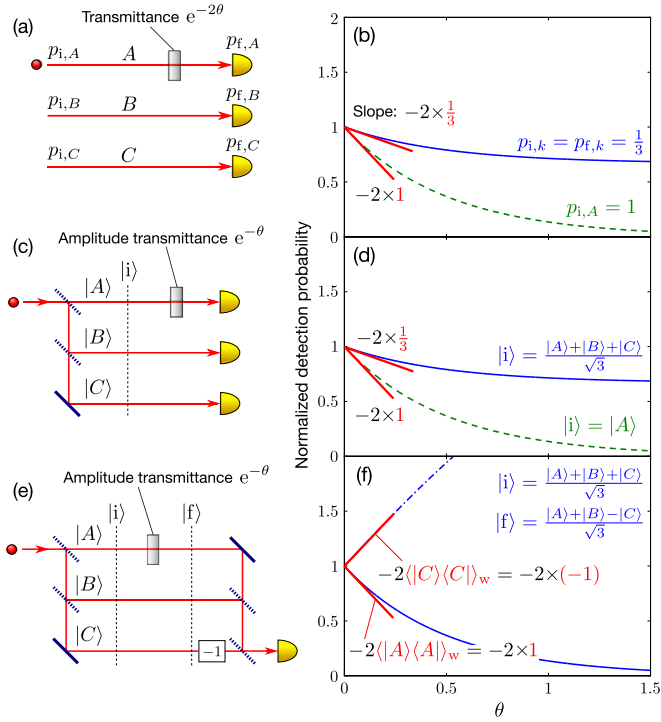
FIG. 5. (a),(b) Pre- and postselected classical system and its normalized detection probability when a probabilistic shutter is set on the path A. The solid blue curve shows that for the case of $p_{i,k} = p_{f,k} = 1/3$ for all k. Its slope at $\theta = 0$, $-2 \times (1/3)$, indicates that the conditional existence probability on the path A of the postselected particle is 1/3. The green dashed curve shows that for the case of $p_{i,A} = 1$ and its slope at $\theta = 0$, -2×1, indicates that the particle has existed on the path A with a probability of 1. (c),(d) Quantum system preselected in $|i\rangle$ and its detection probability when an attenuator is set on the path A. The solid blue curve and green dashed curve show those for the case of $|i\rangle = (|A\rangle + |B\rangle + |C\rangle)/\sqrt{3}$ and $|i\rangle = |A\rangle$, respectively. As in graph (b), their slopes at $\theta = 0$ indicate the conditional existence probability on the path A. (e) Quantum system pre- and postselected in $|i\rangle = (|A\rangle + |B\rangle + |C\rangle)/\sqrt{3}$ and $|f\rangle = (|A\rangle + |B\rangle - |C\rangle)/\sqrt{3}$, respectively. (f) Normalized detection probabilities when an attenuator is set on the path A (solid blue curve) and C (dash-dot blue curve). The slope of the solid blue curve at $\theta = 0$ is -2×1, which looks as if the particle has existed on the path A with a probability of 1. The slope of the dash-dot blue curve at $\theta = 0$ is $-2 \times (-1)$, which looks as if a "negative" particle has existed on the path C.

is detected in path j with a probability of $p_{f,j}$ at postselection. The detection probability $P(f|i)$ is given as

$$P(f|i) = p_{i,A}p_{f,A} + p_{i,B}p_{f,B} + p_{i,C}p_{f,C}. \qquad (24)$$

Next, we put a probabilistic shutter, which passes the particle with a probability of $e^{-2\theta}$ (θ is a non-negative real parameter) on the path k. In this case, the detection probability $P(f|i, k, \theta)$ is given as

$$P(f|i, k, \theta) = P(f|i) - (1 - e^{-2\theta})p_{i,k}p_{f,k}. \qquad (25)$$

The normalized detection probability $P(f|i, k, \theta)/P(f|i)$ has the following derivative with respect to θ at $\theta = 0$:

$$\frac{d}{d\theta} \frac{P(f|i, k, \theta)}{P(f|i)}\bigg|_{\theta=0} = -2\frac{p_{i,k}p_{f,k}}{P(f|i)}. \qquad (26)$$

The right-hand side $[p_{i,k}p_{f,k}/P(f|i)]$ means the conditional existence probability on the path k of the postselected particles, and it appears in the sensitivity of the normalized detection probability $[P(f|i, k, \theta)/P(f|i)]$ with respect to θ at $\theta = 0$. The relation between $P(f|i, A, \theta)/P(f|i)$ and $p_{i,A}p_{f,A}/P(f|i)$ is depicted in Fig. 5(b). For example, when $p_{i,k} = p_{f,k} = 1/3$ for all k, the particle's conditional existence probability is $1/3$, and the variation of $P(f|i, A, \theta)/P(f|i)$ (blue solid curve) has a slope of $-2 \times (1/3)$ at $\theta = 0$. In another example, when $p_{i,A} = 1$, the particle has existed on the path A with a probability of 1, and the variation of $P(f|i, A, \theta)/P(f|i)$ (green dashed curve) has a slope of -2×1 at $\theta = 0$. These results can be intuitively understood: a path with a higher existence probability should be more affected by the shutter, and the reduction rate of the normalized detection probability should be larger.

This intuitive relation also holds for preselected quantum systems. Next, we consider the quantum system preselected in $|i\rangle$ shown in Fig. 5(c). Because postselection is not performed, the detection probability is $P(f|i) = \||i\rangle\|^2 = 1$. The filter on the path k with amplitude transmittance $e^{-\theta}$, which corresponds to the probabilistic shutter in the classical case, is represented as an attenuation transformation $\exp(-\theta|k\rangle\langle k|)$. The detection probability $P(f|i, k, \theta)$ is given as

$$P(f|i, k, \theta) = \|\exp(-\theta|k\rangle\langle k|)|i\rangle\|^2$$
$$= 1 - (1 - e^{-2\theta})\langle i|k\rangle\langle k|i\rangle \qquad (27)$$

and the derivative of the normalized detection probability $P(f|i, k, \theta)/P(f|i)$ with respect to θ at $\theta = 0$ is given as

$$\frac{d}{d\theta} \frac{P(f|i, k, \theta)}{P(f|i)}\bigg|_{\theta=0} = \frac{d}{d\theta} \frac{\|\exp(-\theta|k\rangle\langle k|)|i\rangle\|^2}{\||i\rangle\|^2}\bigg|_{\theta=0}$$
$$= -2\langle i|k\rangle\langle k|i\rangle. \qquad (28)$$

Therefore, the existence probability of the particle on the path k ($\langle i|k\rangle\langle k|i\rangle$) appears in the sensitivity of the normalized detection probability $[P(f|i, k, \theta)/P(f|i)]$ with respect to θ at $\theta = 0$, as mentioned in Sec. II D. The relation between $P(f|i, A, \theta)/P(f|i)$ and $\langle i|A\rangle\langle A|i\rangle$ is depicted in Fig. 5(d). The variation of $P(f|i, A, \theta)/P(f|i)$ when $|i\rangle = (|A\rangle + |B\rangle + |C\rangle)/\sqrt{3}$ (solid blue curve) and $|i\rangle = |A\rangle$ (green dashed curve) show the same curves as those of the classical system in Fig. 5(b).

Finally, we consider the quantum system pre- and postselected in $|i\rangle$ and $|f\rangle$, respectively, shown in Fig. 5(e). The detection probability with the attenuation filter on the path k is represented as

$$P(f|i, k, \theta) = |\langle f|\exp(-\theta|k\rangle\langle k|)|i\rangle|^2$$
$$= |\langle f|i\rangle|^2[1 - (1 - e^{-\theta})2\,\mathrm{Re}\langle k\rangle\langle k|\rangle_w$$
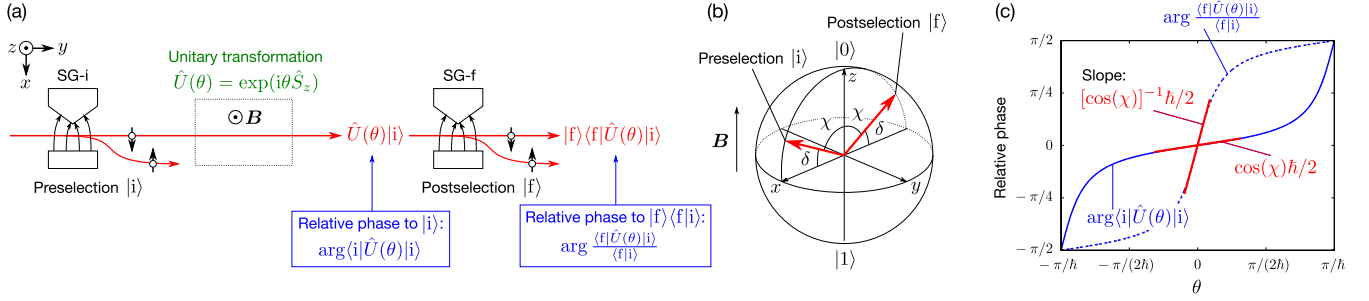$$+ (1 - e^{-\theta})^2|\langle k\rangle\langle k|\rangle_w|^2]. \qquad (29)$$

FIG. 6. (a) Schematic setup considered in Sec. III B. The spin-1/2 particles are pre- and postselected in $|i\rangle$ and $|f\rangle$ by the Stern-Gerlach devices SG-i and SG-f, respectively. Between the pre- and postselection, the particles undergo a unitary transformation $\hat{U}(\theta) = \exp(i\theta\hat{S}_z)$ by a uniform magnetic field in z direction. θ corresponds to the strength of the unitary transformation, which includes the interaction time t and the strength of the magnetic field B. The particles' states before the postselection, $\hat{U}(\theta)|i\rangle$ and $|i\rangle$, show the relative phase $\arg\langle i|\hat{U}(\theta)|i\rangle$, and those after the postselection, $|f\rangle\langle f|\hat{U}(\theta)|i\rangle$ and $|f\rangle\langle f|i\rangle$, show the relative phase $\arg[\langle f|\hat{U}(\theta)|i\rangle/\langle f|i\rangle]$. (b) Bloch sphere representation of the pre- and postselected states. When δ is small, the pre- and postselected states are nearly orthogonal. (c) Variation of the relative phases $\arg\langle i|\hat{U}(\theta)|i\rangle$ (blue solid line) and $\arg[\langle f|\hat{U}(\theta)|i\rangle/\langle f|i\rangle]$ (blue dashed line) when $\chi = 7\pi/16$ ($\delta = \pi/16$). The slope of $\arg\langle i|\hat{U}(\theta)|i\rangle$ at $\theta = 0$ corresponds to the expectation value of the spin angular momentum for $|i\rangle$: $\cos(\chi)\hbar/2 \in [-\hbar/2, \hbar/2]$. The slope of $\arg[\langle f|\hat{U}(\theta)|i\rangle/\langle f|i\rangle]$ at $\theta = 0$ is $[\cos(\chi)]^{-1}\hbar/2 \approx \delta^{-1}\hbar/2$, which becomes arbitrarily large when δ is small. When this slope is identified with their spin angular momentum, it seems like the postselected particles have a huge spin angular momentum.

The derivative of the normalized detection probability $P(f|i, k, \theta)/P(f|i)$ with respect to θ at $\theta = 0$ is given as

$$\left.\frac{d}{d\theta}\frac{P(f|i, k, \theta)}{P(f|i)}\right|_{\theta=0} = -2\,\mathrm{Re}\langle|k\rangle\langle k|\rangle_w, \qquad (30)$$

which has the same form as Eq. (12) in which $\hat{C} = -|k\rangle\langle k|$. The weak probability on the path k ($\langle|k\rangle\langle k|\rangle_w$) appears in the rate of change of the normalized detection probability $[P(f|i, k, \theta)/P(f|i)]$ with respect to θ at $\theta = 0$. By identifying Eq. (30) with Eqs. (26) and (28), the weak probability can be understood in the same manner as the ordinary existence probability of the particle. When $|i\rangle = (|A\rangle + |B\rangle + |C\rangle)/\sqrt{3}$ and $|f\rangle = (|A\rangle + |B\rangle - |C\rangle)/\sqrt{3}$, the variation of $P(f|i, k, \theta)/P(f|i)$ for $k = A$ and C are illustrated as the solid and dash-dot blue curves, respectively, in Fig. 5(f). The solid blue curve, whose slope at $\theta = 0$ is -2×1, has the same shape as the green dashed lines in Figs. 5(b) and 5(d); therefore, the variation of $P(f|i, A, \theta)/P(f|i)$ looks as if the particle exists on path A with a probability of 1. The same argument holds for the path B. In contrast, the dash-dot blue curve, whose slope at $\theta = 0$ is $-2 \times (-1)$, has no counterparts in the classical and preselected quantum systems. The normalized detection probability $P(f|i, C, \theta)/P(f|i)$ is amplified despite the attenuation transformation $\exp(-\theta|C\rangle\langle C|)$, and it looks as if a "negative" particle exists on the path C [29]. In this manner, the strange weak probabilities can be understood in a similar way as the correspondence between the particle's conditional existence probability and the response of the detection probability to an attenuation transformation in classical or preselected quantum systems.

B. Case of the large weak value of the spin of a spin-1/2 particle

In the seminal paper of weak values [1], Aharonov *et al.* proposed that the weak value of the spin z of a spin-1/2 particle can be $100\hbar$ under appropriate pre- and postselection. We next analyze this huge spin weak value using a small unitary transformation, as an example of the case where the real part of the weak value appears in the sensitivity of the ar-

gument of the postselection probability amplitude mentioned in Sec. II C. Based on our formulation of weak values, we explain that this huge spin weak value can also be observed in the change of the spin system itself under a magnetic field, in a method similar to the expectation value of the spin angular momentum in a preselected-only spin system. Note that their classical counterpart is not considered here because the argument cannot be defined in the classical system.

First, we consider that a spin-1/2 system preselected in $|i\rangle$ interacts slightly with the z-directional uniform constant magnetic field B as shown in Fig. 6(a). $\hat{S}_z$ is the z-directional spin operator of a spin-1/2 particle, and $|0\rangle$ and $|1\rangle$ are the eigenstates of $\hat{S}_z$ for eigenvalues $+\hbar/2$ and $-\hbar/2$, respectively. The interaction Hamiltonian is $\hat{H} = -\gamma\hat{S}_zB$, where γ is the gyromagnetic ratio, and the time evolution unitary operator for time t is $\exp(i\gamma\hat{S}_zBt/\hbar) = \exp(i\theta\hat{S}_z) =: \hat{U}(\theta)$, where $\theta := \gamma Bt/\hbar$. After the interaction, the spin state is transformed into $\hat{U}(\theta)|i\rangle$. While the unitary transformation $\hat{U}(\theta)$ does not change the norm of $\hat{U}(\theta)|i\rangle$, the global phase of $\hat{U}(\theta)|i\rangle$ changes depending on the spin z component of $|i\rangle$. The relative phase of $\hat{U}(\theta)|i\rangle$ to $|i\rangle$ shows the following relations:

$$\frac{d}{d\theta}\arg\langle i|[\hat{U}(\theta)|i\rangle]|_{\theta=0} = \mathrm{Im}\langle i|(i\hat{S}_z)|i\rangle = \langle i|\hat{S}_z|i\rangle. \qquad (31)$$

Therefore, the expectation value of $\hat{S}_z$ for the preselected state $|i\rangle$ ($\langle i|\hat{S}_z|i\rangle$) appears in the sensitivity to θ of the relative phase of $\hat{U}(\theta)|i\rangle$ to $|i\rangle$ [$\arg\langle i|\hat{U}(\theta)|i\rangle$] under an external effect (the magnetic field), as mentioned in Sec. II D. The variation of $\arg\langle i|\hat{U}(\theta)|i\rangle$ for $|i\rangle = \cos(\chi/2)|0\rangle + \sin(\chi/2)|1\rangle$ ($\chi \in [0, \pi]$) is shown in Fig. 6(c). Its slope at $\theta = 0$ is $\langle i|\hat{S}_z|i\rangle = \cos(\chi)\hbar/2$, which is bounded in the range of the eigenvalues of $\hat{S}_z$, $[-\hbar/2, \hbar/2]$.

Next, we consider a spin-1/2 system pre- and postselected in $|i\rangle$ and $|f\rangle$, respectively, as shown in Fig. 6(a). The postselected (unnormalized) state becomes $|f\rangle\langle f|\hat{U}(\theta)|i\rangle$, and its

relative phase to $|f\rangle\langle f|i\rangle$ shows the following relations:

$$\frac{d}{d\theta}\arg[\langle i|f\rangle\langle f|][|f\rangle\langle f|\hat{U}(\theta)|i\rangle]]|_{\theta=0} = \frac{d}{d\theta}\arg\frac{\langle f|\hat{U}(\theta)|i\rangle}{\langle f|i\rangle}\Big|_{\theta=0}$$

$$= \mathrm{Re}\langle\hat{S}_z\rangle_{\mathrm{w}}. \qquad (32)$$

Equation (32) has the same form as that of Eq. (7) in which $\hat{C} = i\hat{S}_z$ and indicates that $\mathrm{Re}\langle\hat{S}_z\rangle_{\mathrm{w}}$ corresponds to the sensitivity to θ of the relative phase of $|f\rangle\langle f|\hat{U}(\theta)|i\rangle$ to $|f\rangle\langle f|i\rangle$ [34]. Unlike $\langle i|\hat{S}_z|i\rangle$ in Eq. (31), $\mathrm{Re}\langle\hat{S}_z\rangle_{\mathrm{w}}$ can be an arbitrary real number. For example, if $|i\rangle = \cos(\chi/2)|0\rangle + \sin(\chi/2)|1\rangle$ and $|f\rangle = \cos(\chi/2)|0\rangle - \sin(\chi/2)|1\rangle$ ($\chi \in [0, \pi]$) as shown in Fig. 6(b), $\mathrm{Re}\langle\hat{S}_z\rangle_{\mathrm{w}} = [\cos(\chi)]^{-1}\hbar/2$. When $\chi = \pi/2 - \delta$ and $0 < \delta \ll 1$, $\mathrm{Re}\langle\hat{S}_z\rangle_{\mathrm{w}} \approx \delta^{-1}\hbar/2$, which is much larger than $\hbar/2$. In this case, the relative phase $\arg[\langle f|\hat{U}(\theta)|i\rangle/\langle f|i\rangle]$ changes sensitively to the change of θ as shown in Fig. 6(c). By identifying Eq. (32) with Eq. (31), the particles look as if they have a huge angular momentum $\delta^{-1}\hbar/2$. In this manner, the huge weak value can be interpreted as a natural extension of the expectation value of the spin angular momentum. We note that the measurement of these relative phases requires an additional degree of freedom as mentioned in Sec. II C.

IV. PERFORMANCE EVALUATION OF WEAK-VALUE MEASUREMENT METHOD WITHOUT USING PROBE SYSTEMS

In the previous sections, we illustrated the conceptual advantage of the proposed operational formulation of weak values so that the strange weak values can be understood directly. Here, we also note that the weak-values measurement method based on this formulation has a practical advantage, i.e., this measurement system can be simplified compared with the original weak measurement. In contrast, the original weak measurement requires the preparation and measurement of the probe system. The measurement of the weak values appearing in the modulus change of the postselection probability amplitude in our formulation can be performed by directly measuring the system and external degrees of freedom are not required. To clarify the applicability of our measurement method to various weak-value measurement experiments, we discuss the following three points. In Sec. IV A, we describe how to apply our measurement method to weak-value amplification. In Sec. IV B, we evaluate the performance of our measurement method as a weak-value estimation method in terms of accuracy and precision. In Sec. IV C, we mention the weak-value measurement methods other than weak measurement previously reported and compare the advantages of these methods and our measurement method.

A. Weak-value amplification in the proposed formulation

Weak-value amplification [11–14], which is one of the most important applications of weak measurement, aims to estimate the interaction strength of a given weak von Neumann interaction between two systems. Because the measurement systems for weak-value amplification inevitably involve probe systems, our measurement method appears not applicable to weak-value amplification directly. In this section, we describe how to apply our measurement method to weak-value amplification.
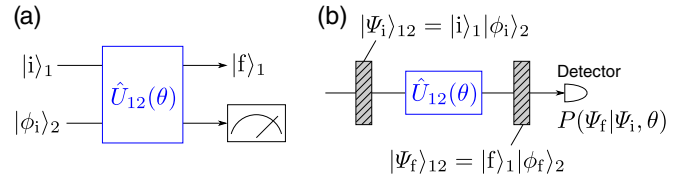

FIG. 7. (a) Quantum system for weak-value amplification. The upper system (system 1) is pre- and postselected in $|i\rangle_1$ and $|f\rangle_1$, respectively. The lower system (system 2) is a probe system preselected in $|\phi_i\rangle_2$ and, after the interaction $\hat{U}_{12}(\theta)$, the probe shift is measured. When $|_1\langle f|i\rangle_1| \ll 1$, $|\langle\hat{A}_1\rangle_{\mathrm{w}}|$ becomes large; therefore, the probe shift can be detected even if θ is very small. (b) Quantum system in our measurement method. Systems 1 and 2 are considered as a composite system pre- and postselected in $|\Psi_i\rangle_{12}$ and $|\Psi_f\rangle_{12}$, respectively. θ is estimated from the variation of the postselection probability $P(\Psi_f|\Psi_i, \theta)$, which can be detected even if θ is very small when $|_{12}\langle\Psi_f|\Psi_i\rangle_{12}| \ll 1$.

As shown in Fig. 7(a), in weak-value amplification, a weak von Neumann interaction between a system to be measured (system 1) and a probe system (system 2) is given, and the unitary transformation caused by this interaction is expressed as $\hat{U}_{12}(\theta) = \exp(i\theta\hat{A}_1 \otimes \hat{A}_2)$, where $\hat{A}_1$ and $\hat{A}_2$ are Hermite operators on the systems 1 and 2, respectively, and θ is a small real parameter to be estimated. To apply our measurement method, we consider the two systems as a composite single system as shown in Fig. 7(b). When the total system is pre- and postselected in $|\Psi_i\rangle_{12} = |i\rangle_1|\phi_i\rangle_2$ and $|\Psi_f\rangle_{12} = |f\rangle_1|\phi_f\rangle_2$, respectively, the ratio of its postselection probability $P(\Psi_f|\Psi_i, \theta)$ for $\theta \neq 0$ to that for $\theta = 0$ is represented as

$$\frac{P(\Psi_f|\Psi_i, \theta)}{P(\Psi_f|\Psi_i, 0)} = \frac{|_{12}\langle\Psi_f|\hat{U}_{12}(\theta)|\Psi_i\rangle_{12}|^2}{|_{12}\langle\Psi_f|\Psi_i\rangle_{12}|^2}$$

$$= 1 + 2\,\mathrm{Re}(i\langle\hat{A}_1\rangle_{\mathrm{w}}\langle\hat{A}_2\rangle_{\mathrm{w}})\theta + O(\theta^2), \qquad (33)$$

where $\langle\hat{A}_1\rangle_{\mathrm{w}} := {}_1\langle f|\hat{A}_1|i\rangle_1/{}_1\langle f|i\rangle_1$ and $\langle\hat{A}_2\rangle_{\mathrm{w}} := {}_2\langle\phi_f|\hat{A}_2|\phi_i\rangle_2/{}_2\langle\phi_f|\phi_i\rangle_2$. When the pre- and postselected states are prepared so that $i\langle\hat{A}_1\rangle_{\mathrm{w}}\langle\hat{A}_2\rangle_{\mathrm{w}}$ becomes a huge real value, the difference $P(\theta)/P(0) - 1$ can be detected experimentally even if θ is very small, and when $\langle\hat{A}_1\rangle_{\mathrm{w}}$ and $\langle\hat{A}_2\rangle_{\mathrm{w}}$ are known, θ can be estimated from the difference $P(\theta)/P(0) - 1$. This is the same strategy as weak-value amplification.

In the conventional weak measurement for weak-value amplification, the amount of the probe shift needs to be measured. For example, optical weak measurement experiments at the single-photon level require a single-photon detector with spatial resolution, such as an electron multiplying CCD camera or an avalanche photodiode array. However, our measurement method can be realized with a relatively inexpensive experimental device such as a photon detector without spatial resolution. Therefore, the implementation of our measurement method is easier than the conventional weak measurement.

B. Accuracy and precision in the proposed measurement method

Here, we evaluate the performance of our measurement method as a weak-value estimation method in terms of the accuracy and precision. First, the accuracy is defined as the difference of the estimator for infinite number of trials from the true value. In our measurement method, Eq. (3) indicates that there is a difference $O(\theta^2)$ between $\langle f|\hat{N}(\theta)|i\rangle/\langle f|i\rangle - 1$ and $\langle \hat{C}\rangle_w\theta$, and the estimator of the weak value for infinite number of trials, $[\langle f|\hat{N}(\theta)|i\rangle/\langle f|i\rangle - 1]/\theta$, contains an error of $O(\theta)$. Nevertheless, the first order term of θ in this error can be canceled by measuring not only $\langle f|\hat{N}(\theta)|i\rangle/\langle f|i\rangle - 1$ but also $\langle f|\hat{N}(-\theta)|i\rangle/\langle f|i\rangle - 1$ and taking the difference between the two as

$$\frac{\langle f|\hat{N}(\theta)|i\rangle}{\langle f|i\rangle} - \frac{\langle f|\hat{N}(-\theta)|i\rangle}{\langle f|i\rangle} = 2\langle \hat{C}\rangle_w\theta + O(\theta^3). \quad (34)$$

If the strength of the transformation θ is known, $\langle \hat{C}\rangle_w$ can be estimated with an error of $O(\theta^2)$ for infinite number of trials. This technique can be used for estimating the real and imaginary part of weak values in Eqs. (11) and (13), respectively, to cancel the first order term of θ in their errors. In weak measurement using a Gaussian probe, the estimation error of a weak value for infinite number of trials can also be reduced to $O(\theta^2)$, where θ is the interaction strength between the measured and probe systems (see Appendix B for details).

Next, the precision is defined as the uncertainty (mean square error deviation) of the estimator for finite number of trials. The lower bound of this estimation uncertainty for n trials, $\Delta\langle \hat{C}\rangle_w$, is given by quantum Cramér-Rao inequality [35] as follows:

$$\Delta\langle \hat{C}\rangle_w \geqslant \frac{1}{\sqrt{nF}} \geqslant \frac{1}{\sqrt{nF_Q}}, \quad (35)$$

where F and F_Q are classical and quantum Fisher information, respectively. When θ is known and $\mathrm{Re}\langle \hat{C}\rangle_w$ is to be estimated, the classical Fisher information of the probability distribution $\{P(f|i, \theta) = |\langle f|\hat{N}(\theta)|i\rangle|^2, 1 - P(f|i, \theta)\}$ is given as

$$F = \frac{4|\langle f|i\rangle|^2}{1 - |\langle f|i\rangle|^2}\theta^2 + O(\theta^3). \quad (36)$$

This value is larger than that for weak measurement using a Gaussian probe (see Appendix B for details) and becomes particularly large when the denominator $1 - |\langle f|i\rangle|^2$ is close to zero. In contrast, when θ is to be estimated, the quantum Fisher information of the state $\hat{N}(\theta)|i\rangle$ is given as

$$F_Q = 4(\langle i|\hat{C}^\dagger\hat{C}|i\rangle - |\langle i|\hat{C}|i\rangle|^2) + O(\theta). \quad (37)$$

If $\hat{C}$ is anti-Hermite [i.e., $\hat{N}(\theta)$ is unitary], the right equality in Eq. (35) holds when the postselected state is chosen as

$$|f\rangle = \frac{1}{\sqrt{2}}\left[|i\rangle + \frac{(\hat{1} - |i\rangle\langle i|)\hat{C}|i\rangle}{\|(\hat{1} - |i\rangle\langle i|)\hat{C}|i\rangle\|}\right]. \quad (38)$$

We note that the weak value $\langle \hat{C}\rangle_w$ is not huge for this $|f\rangle$, which indicates that the strategy of weak-value amplification is not optimal for such an ideal situation, similar to the results in the previous studies [36–38]. Nevertheless, there is a possibility that weak-value amplification becomes an

optimal strategy under the presence of a specific technical noise [39–41].

C. Other weak-value measurement methods

While our measurement method is an alternative to weak measurement to obtain weak values, some other weak-value measurement methods have been proposed so far [42–49]. Here, we mention these weak-value measurement methods other than weak measurement and compare the advantages of each method and our measurement method.

Some of the methods previously reported [42–47] employ indirect (von Neumann) measurement via strong system-probe interactions. The others [48,49] are direct measurement methods, in which weak values are obtained from a combination of several projective (strong) measurements of preselected systems. These methods have an advantage over weak measurement in terms of efficiency because of the strong interactions or measurements, while the pre- and postselected systems are strongly disturbed. Therefore, these methods can be applied to, for example, direct measurements of wave functions and pseudoprobability distributions of the system's preselected state [15–22].

In contrast, the characteristic of hardly disturbing measured pre- and postselected systems, which weak measurement has, is essential for the studies that have investigated physical quantities of quantum systems after postselection by weak measurement [3–10] and weak-value amplification [11–14]. Our weak-value measurement method also maintains the characteristic of hardly disturbing the pre- and postselected systems because the weak values are obtained at the limit of very small transformation. Therefore, our measurement method is widely applicable to such applications instead of weak measurement.

V. CONCLUSION

In this study, we proposed an operational formulation of weak values as the response of the pre- and postselected system, without using probe systems. In this formulation, when a small quantum transformation is given between the pre- and postselections, the weak value of the generator of this small transformation appears in the change of the postselection probability amplitude. This formulation is a generalization of the results that have been reported before and therefore covers various cases, such as when the small transformation is other than unitary or attenuation transformations, or when the pre- and postselection is in a mixed state. We applied this formulation to examples of the quantum box problem and the huge weak value of spin to provide a direct interpretation of the strange weak values as a natural extension of the conventional physical quantities such as probability and spin angular momentum. In addition, we explained that the measurement of the weak values appearing in the modulus change of the postselection probability amplitude in this formulation, which does not require external degrees of freedom, can be applied to simplify various weak-value measurement experiments. Thus the proposed operational formulation of weak values, freed from the concept of probe shift, is expected to play an

important role in both fundamental and practical investigation on weak values and pre- and postselection quantum systems.

APPENDIX A: HOW TO REALIZE AMPLIFICATION OR ATTENUATION TRANSFORMATION

In this Appendix, we describe how to realize the small amplification or attenuation transformation by unitary processes. While the time evolution of closed systems must be unitary in quantum mechanics, the small amplification or attenuation transformation in a target space can be realized effectively by embedding that transformation into a unitary transformation on a dilated space, as shown below. Let us consider the target d-dimensional Hilbert space $\mathcal{H}$ and a dilated $(d + d')$-dimensional Hilbert space $\mathcal{H} \oplus \mathcal{H}'$, where $\mathcal{H}'$ is an additional d'-dimensional Hilbert space satisfying $\mathcal{H}' \perp \mathcal{H}$. The initial state $k(|i\rangle + |\chi_i\rangle)$, where $|i\rangle \in \mathcal{H}$, $|\chi_i\rangle \in \mathcal{H}'$, and $k = 1/\sqrt{\langle i|i\rangle + \langle \chi_i|\chi_i\rangle}$, undergoes unitary evolution $\hat{U}(\theta) = \hat{1} + i\theta\hat{A} + O(\theta^2)$, where $\hat{A}$ is a Hermite operator on $\mathcal{H} \oplus \mathcal{H}'$ and then is projected onto $\mathcal{H}$ by $\hat{P} := \hat{1}_{\mathcal{H}} \oplus 0_{\mathcal{H}'}$. $\hat{A}$ is represented as $\hat{A} = \begin{bmatrix} \hat{A}_{11} & \hat{A}_{12} \\ \hat{A}_{21} & \hat{A}_{22} \end{bmatrix}$, where $\hat{A}_{11} : \mathcal{H} \to \mathcal{H}$ and $\hat{A}_{22} : \mathcal{H}' \to \mathcal{H}'$ are Hermite operators and $\hat{A}_{12} : \mathcal{H}' \to \mathcal{H}$ and $\hat{A}_{21} : \mathcal{H} \to \mathcal{H}'$ satisfy $\hat{A}_{12}^\dagger = \hat{A}_{21}$ due to the Hermitian condition $\hat{A}^\dagger = \hat{A}$. The resulting state after the transformation is given as

$$\hat{P}\hat{U}(\theta)k(|i\rangle + |\chi_i\rangle) = (\hat{1} + i\theta\hat{A}_{11})k|i\rangle + i\theta\hat{A}_{12}k|\chi_i\rangle + O(\theta^2). \tag{A1}$$

The first term of the right-hand side, $(\hat{1} + i\theta\hat{A}_{11})k|i\rangle$, represents the unitary evolution in $\mathcal{H}$, and the second term, $i\theta\hat{A}_{12}k|\chi_i\rangle \in \mathcal{H}$, represents the inflow of the amplitude from $\mathcal{H}'$ to $\mathcal{H}$. Therefore, if $\hat{A}_{11} = 0$ and $i\theta\hat{A}_{12}k|\chi_i\rangle$ is represented as $\hat{B}k|i\rangle$, the amplification or attenuation transformation $\hat{1} + \theta\hat{B} + O(\theta^2)$ for the state $k|i\rangle$ is effectively realized.

Another way to realize an amplification or attenuation transformation is using an interaction with an ancilla system. Let us consider a weak von Neumann interaction between a system to be measured (system 1) and a probe system (system 2) expressed as $\exp(i\theta\hat{A}_1 \otimes \hat{A}_2)$, where $\hat{A}_1$ and $\hat{A}_2$ are Hermite operators on the systems 1 and 2, respectively. When the system 2 is pre- and postselected in $|\phi_i\rangle_2$ and $|\phi_f\rangle_2$, respectively, the system 1 undergoes the following effective small transformation:

$$_2\langle\phi_f|\exp(i\theta\hat{A}_1 \otimes \hat{A}_2)|\phi_i\rangle_2$$
$$= {}_2\langle\phi_f|\phi_i\rangle_2[1 + \theta(i\langle\hat{A}_2\rangle_w\hat{A}_1) + O(\theta^2)], \tag{A2}$$

where $\langle\hat{A}_2\rangle_w := {}_2\langle\phi_f|\hat{A}_2|\phi_i\rangle_2/{}_2\langle\phi_f|\phi_i\rangle_2$. If $\langle\hat{A}_2\rangle_w$ is real, the effective small transformation becomes a unitary transformation whose generator is an anti-Hermite operator $i\langle\hat{A}_2\rangle_w\hat{A}_1$.

In contrast, if $\langle\hat{A}_2\rangle_w$ is purely imaginary, the effective small transformation becomes an amplification or attenuation transformation whose generator is a Hermite operator $i\langle\hat{A}_2\rangle_w\hat{A}_1$. We note that the case where the norm of the state vector of system 1 exceeds one because of the effective amplification transformation is understood as follows: the postselection probability for system 2 becomes larger than $|_2\langle\phi_f|\phi_i\rangle_2|^2$; therefore, the number of trials of system 1 that remains after the postselection of system 2 is increased.

APPENDIX B: ACCURACY AND PRECISION IN WEAK MEASUREMENT USING A GAUSSIAN PROBE

In this Appendix, we provide the accuracy and precision in weak measurement using a Gaussian probe. Before that, we review the weak measurement using a Gaussian probe. The initial states of the measured and probe systems are $|i\rangle$ and $|\phi\rangle$, respectively. We assume that $|\phi\rangle$ can be expanded in the position basis $\{|x\rangle\}$ as

$$|\phi\rangle = \int_{-\infty}^{\infty} dx\,\phi(x)|x\rangle, \quad \phi(x) = \frac{1}{\pi^{1/4}\sqrt{\sigma}}\exp\frac{-x^2}{2\sigma^2}. \tag{B1}$$

The initial state $|i\rangle|\phi\rangle$ is evolved through the weak system-probe interaction $\exp(-i\theta\hat{A} \otimes \hat{p})$, where $\hat{A}$ is the measured observable, $\hat{p}$ is the momentum operator of the probe system, and θ is a small coupling constant satisfying $\theta\|\hat{A}\| \ll \sigma$ ($\|\hat{A}\|$ is the maximum eigenvalue of $\hat{A}$). After the system is postselected into $|f\rangle$, the un-normalized state of the probe system $|\tilde{\phi}_f\rangle$ is represented as

$$|\tilde{\phi}_f\rangle = \langle f|\exp(-i\theta\hat{A} \otimes \hat{p})|i\rangle|\phi\rangle$$
$$= \langle f|i\rangle\left(\hat{1} - i\theta\langle\hat{A}\rangle_w\hat{p} - \frac{\theta^2}{2}\langle\hat{A}^2\rangle_w\hat{p}^2\right)|\phi\rangle + O(\theta^3). \tag{B2}$$

The projection measurement of the position $\{|x\rangle\langle x|\}$ for $|\tilde{\phi}_f\rangle$ gives the following probability density distribution $P(x|\text{Re}\langle\hat{A}\rangle_w)$:

$$P(x|\text{Re}\langle\hat{A}\rangle_w) = \frac{\langle\tilde{\phi}_f|x\rangle\langle x|\tilde{\phi}_f\rangle}{\langle\tilde{\phi}_f|\tilde{\phi}_f\rangle}$$
$$= |\phi(x)|^2\left[1 + \frac{2\,\text{Re}\langle\hat{A}\rangle_w x}{\sigma^2}\theta \right.$$
$$\left. + \frac{|\langle\hat{A}\rangle_w|^2 + \text{Re}\langle\hat{A}^2\rangle_w}{2\sigma^2}\left(\frac{x^2}{\sigma^2} - \frac{1}{2}\right)\theta^2\right]$$
$$+ O(\theta^3). \tag{B3}$$

In weak measurement, $\text{Re}\langle\hat{A}\rangle_w$ is estimated as the averaged value of the outcomes of the position measurement to the probe system. For an infinite number of trials, the estimator of $\text{Re}\langle\hat{A}\rangle_w$ is given as the expectation value of the probability density distribution $P(x|\text{Re}\langle\hat{A}\rangle_w)$, which is represented as

$$\int_{-\infty}^{\infty} dx\,P(x|\text{Re}\langle\hat{A}\rangle_w) = \theta\,\text{Re}\langle\hat{A}\rangle_w + O(\theta^3). \tag{B4}$$

Therefore, $\text{Re}\langle\hat{A}\rangle_w$ can be estimated with an error of $O(\theta^2)$ for an infinite number of trials.

The classical Fisher information of the probability density distribution $P(x|\mathrm{Re}\langle\hat{A}\rangle_\mathrm{w})$ is given as

$$J = \int_{-\infty}^{\infty} dx \frac{1}{P(x|\mathrm{Re}\langle\hat{A}\rangle_\mathrm{w})} \left[\frac{dP(x|\mathrm{Re}\langle\hat{A}\rangle_\mathrm{w})}{d(\mathrm{Re}\langle\hat{A}\rangle_\mathrm{w})}\right]^2 = |\langle\mathrm{f}|\mathrm{i}\rangle|^2 \theta'^2 + O(\theta'^3), \tag{B5}$$

where $\theta' := \theta/\sigma$ is the parameter representing the substantial strength of the interaction.

[1] Y. Aharonov, D. Z. Albert, and L. Vaidman, How the Result of a Measurement of a Component of the Spin of a Spin-1/2 Particle Can Turn Out to be 100, Phys. Rev. Lett. **60**, 1351 (1988).

[2] R. Jozsa, Complex weak values in quantum measurement, Phys. Rev. A **76**, 044103 (2007).

[3] Y. Aharonov and L. Vaidman, Complete description of a quantum system at a given time, J. Phys. A **24**, 2315 (1991).

[4] K. J. Resch, J. S. Lundeen, and A. M. Steinberg, Experimental realization of the quantum box problem, Phys. Lett. A **324**, 125 (2004).

[5] J. S. Lundeen and A. M. Steinberg, Experimental Joint Weak Measurement on a Photon Pair as a Probe of Hardy's Paradox, Phys. Rev. Lett. **102**, 020404 (2009).

[6] K. Yokota, T. Yamamoto, M. Koashi, and N. Imoto, Direct observation of Hardy's paradox by joint weak measurement with an entangled photon pair, New J. Phys. **11**, 033011 (2009).

[7] S. Kocsis, B. Braverman, S. Ravets, M. J. Stevens, R. P. Mirin, L. K. Shalm, and A. M. Steinberg, Observing the average trajectories of single photons in a two-slit interferometer, Science **332**, 1170 (2011).

[8] M. E. Goggin, M. P. Almeida, M. Barbieri, B. P. Lanyon, J. L. O'Brien, A. G. White, and G. J. Pryde, Violation of the Leggett-Garg inequality with weak measurements of photons, Proc. Natl. Acad. Sci. USA **108**, 1256 (2011).

[9] T. Denkmayr, H. Geppert, S. Sponar, H. Lemmel, A. Matzkin, J. Tollaksen, and Y. Hasegawa, Observation of a quantum cheshire cat in a matter-wave interferometer experiment, Nat. Commun. **5**, 4492 (2014).

[10] D. H. Mahler, L. Rozema, K. Fisher, L. Vermeyden, K. J. Resch, H. M. Wiseman, and A. M. Steinberg, Experimental nonlocal and surreal Bohmian trajectories, Sci. Adv. **2**, e1501466 (2016).

[11] O. Hosten and P. Kwiat, Observation of the spin Hall effect of light via weak measurements, Science **319**, 787 (2008).

[12] P. B. Dixon, D. J. Starling, A. N. Jordan, and J. C. Howell, Ultrasensitive Beam Deflection Measurement via Interferometric Weak Value Amplification, Phys. Rev. Lett. **102**, 173601 (2009).

[13] O. S. Magaña-Loaiza, M. Mirhosseini, B. Rodenburg, and R. W. Boyd, Amplification of Angular Rotations Using Weak Measurements, Phys. Rev. Lett. **112**, 200401 (2014).

[14] M. Hallaji, A. Feizpour, G. Dmochowski, J. Sinclair, and A. M. Steinberg, Weak-value amplification of the nonlinear effect of a single photon, Nat. Phys. **13**, 540 (2017).

[15] J. S. Lundeen, B. Sutherland, A. Patel, C. Stewart, and C. Bamber, Direct measurement of the quantum wavefunction, Nature (London) **474**, 188 (2011).

[16] J. S. Lundeen and C. Bamber, Procedure for Direct Measurement of General Quantum States Using Weak Measurement, Phys. Rev. Lett. **108**, 070402 (2012).

[17] J. Z. Salvail, M. Agnew, A. S. Johnson, E. Bolduc, J. Leach, and R. W. Boyd, Full characterization of polarization states of light via direct measurement, Nat. Photon. **7**, 316 (2013).

[18] H. Kobayashi, K. Nonaka, and Y. Shikano, Stereographical visualization of a polarization state using weak measurements with an optical-vortex beam, Phys. Rev. A **89**, 053816 (2014).

[19] M. Malik, M. Mirhosseini, M. P. J. Lavery, J. Leach, M. J. Padgett, and R. W. Boyd, Direct measurement of a 27-dimensional orbital-angular-momentum state vector, Nat. Commun. **5**, 3115 (2014).

[20] M. Mirhosseini, O. S. Magaña-Loaiza, S. M. Hashemi Rafsanjani, and R. W. Boyd, Compressive Direct Measurement of the Quantum Wave Function, Phys. Rev. Lett. **113**, 090402 (2014).

[21] Z. Shi, M. Mirhosseini, J. Margiewicz, M. Malik, F. Rivera, Z. Zhu, and R. W. Boyd, Scan-free direct measurement of an extremely high-dimensional photonic state, Optica **2**, 388 (2015).

[22] G. S. Thekkadath, L. Giner, Y. Chalich, M. J. Horton, J. Banker, and J. S. Lundeen, Direct Measurement of the Density Matrix of a Quantum System, Phys. Rev. Lett. **117**, 120401 (2016).

[23] A. Hosoya and Y. Shikano, Strange weak values, J. Phys. A **43**, 385307 (2010).

[24] The weak value can be determined using Eq. (1) only when both the pre- and postselected system and the measured observable are known, regardless of the existence of a probe system. Hence weak values certainly belong to the pre- and postselected system; however, to measure their quantity, it is necessary to choose the measured observable.

[25] We use the notation $O(f(\theta))$ as an operator satisfying $\limsup_{\theta\to 0}||O(f(\theta))/f(\theta)|| < \infty$, where $||\cdot||$ is an operator norm.

[26] We used the following relations for any complex functions $f(\theta)$ satisfying $f(0) = 1$:

$$|f(\theta)| = \mathrm{Re}f(\theta) + O(\theta^2), \tag{6}$$

$$\arg f(\theta) = \mathrm{Im}f(\theta) + O(\theta^2). \tag{7}$$

[27] S. Pancharatnam, Generalized theory of interference and its applications, Proc. Ind. Acad. Sci. A **44**, 398 (1956).

[28] H. F. Hofmann, Uncertainty limits for quantum metrology obtained from the statistics of weak measurements, Phys. Rev. A **83**, 022106 (2011).

[29] K. Yokota, The real and imaginary parts of a weak value appearing as back-actions via a post-selection, arXiv:1909.04806.

[30] L. B. Ho and N. Imoto, An interpretation and understanding of complex modular values, arXiv:1602.01594.

[31] J. Dressel, M. Malik, F. M. Miatto, A. N. Jordan, and R. W. Boyd, Colloquium: Understanding quantum weak values: Basics and applications, Rev. Mod. Phys. **86**, 307 (2014).

[32] X. Qiu, L. Xie, X. Liu, L. Luo, Z. Li, Z. Zhang, and J. Du, Precision phase estimation based on weak-value amplification, Appl. Phys. Lett. **110**, 071105 (2017).

[33] M. Cormann, M. Remy, B. Kolaric, and Y. Caudano, Revealing geometric phases in modular and weak values with a quantum eraser, Phys. Rev. A **93**, 042124 (2016).

[34] S. Tamate, H. Kobayashi, T. Nakanishi, K. Sugiyama, and M. Kitano, Geometrical aspects of weak measurements and quantum erasers, New J. Phys. **11**, 093025 (2009).

[35] S. L. Braunstein and C. M. Caves, Statistical Distance and the Geometry of Quantum States, Phys. Rev. Lett. **72**, 3439 (1994).

[36] S. Tanaka and N. Yamamoto, Information amplification via postselection: A parameter-estimation perspective, Phys. Rev. A **88**, 042116 (2013).

[37] C. Ferrie and J. Combes, Weak Value Amplification is Suboptimal for Estimation and Detection, Phys. Rev. Lett. **112**, 040406 (2014).

[38] L. Zhang, A. Datta, and I. A. Walmsley, Precision Metrology Using Weak Measurements, Phys. Rev. Lett. **114**, 210801 (2015).

[39] J. Harris, R. W. Boyd, and J. S. Lundeen, Weak Value Amplification can Outperform Conventional Measurement in the Presence of Detector Saturation, Phys. Rev. Lett. **118**, 070802 (2017).

[40] A. N. Jordan, J. Martínez-Rincón, and J. C. Howell, Technical Advantages for Weak-Value Amplification: When Less is More, Phys. Rev. X **4**, 011031 (2014).

[41] G. I. Viza, J. Martínez-Rincón, G. B. Alves, A. N. Jordan, and J. C. Howell, Experimentally quantifying the advantages of weak-value-based metrology, Phys. Rev. A **92**, 032127 (2015).

[42] G. Vallone and D. Dequal, Strong Measurements Give a Better Direct Measurement of the Quantum Wave Function, Phys. Rev. Lett. **116**, 040502 (2016).

[43] T. Denkmayr, H. Geppert, H. Lemmel, M. Waegell, J. Dressel, Y. Hasegawa, and S. Sponar, Experimental Demonstration of Direct Path State Characterization by Strongly Measuring Weak Values in a Matter-Wave Interferometer, Phys. Rev. Lett. **118**, 010402 (2017).

[44] Y. Kedem and L. Vaidman, Modular Values and Weak Values of Quantum Observables, Phys. Rev. Lett. **105**, 230401 (2010).

[45] H. F. Hofmann, Sequential measurements of non-commuting observables with quantum controlled interactions, New J. Phys. **16**, 063056 (2014).

[46] K. Ogawa, O. Yasuhiko, H. Kobayashi, T. Nakanishi, and A. Tomita, A framework for measuring weak values without weak interactions and its diagrammatic representation, New J. Phys. **21**, 043013 (2019).

[47] L. Calderaro, G. Foletto, D. Dequal, P. Villoresi, and G. Vallone, Direct Reconstruction of the Quantum Density Matrix by Strong Measurements, Phys. Rev. Lett. **121**, 230501 (2018).

[48] L. M. Johansen, Reconstructing weak values without weak measurements, Phys. Lett. A **366**, 374 (2007).

[49] E. Cohen and E. Pollak, Determination of weak values of quantum operators using only strong measurements, Phys. Rev. A **98**, 042112 (2018).